High-redshift formation and evolution of central massive objects – II. The census of BH seeds

B. Devecchi,[1]* M. Volonteri,[2] E. M. Rossi,[1] M. Colpi[3] and S. Portegies Zwart[1]

[1]*Leiden Observatory, Leiden University, PO Box 9513, 2300 RA Leiden, the Netherlands*
[2]*Astronomy Department, University of Michigan, 500 Church Street, Ann Arbor, MI 48109, USA*
[3]*Dipartimento di Fisica G. Occhialini, Università degli Studi di Milano Bicocca, Piazza della Scienza 3, 20126 Milano, Italy*

ABSTRACT

We present results of simulations aimed at tracing the formation of nuclear star clusters (NCs) and black hole (BH) seeds in the framework of the current Λcold dark matter (ΛCDM) cosmogony. These BH seeds are considered to be progenitors of the supermassive BHs that inhabit today's galaxies. We focus on two mechanisms for the formation of BHs at high redshifts: as end-products of (1) Population III stars in metal-free haloes, and (2) runaway stellar collisions in metal-poor NCs. Our model tracks the chemical, radiative and mechanical feedback of stars on the baryonic component of the evolving haloes. This procedure allows us to evaluate *when* and *where* the conditions for BH formation are met, and to trace the emergence of BH seeds arising from the dynamical channel, in a cosmological context. BHs start to appear already at redshift $\sim$30 as remnants of Population III stars. The efficiency of this mechanism begins decreasing once feedbacks become increasingly important. Around redshift $z \sim 15$, BHs mostly form in the centre of mildly metal-enriched haloes inside dense NCs. The seed BHs that form along the two pathways have at birth a mass of around 100–1000 $M_\odot$. The occupation fraction of BHs is a function of both halo mass and mass growth rate: at a given redshift, heavier and faster growing haloes have a higher chance to form a *native* BH, or to acquire an *inherited* BH via merging of another system. With decreasing z, the probability of finding a BH shifts towards progressively higher mass halo intervals. This is due to the fact that, at later cosmic times, low-mass systems rarely form a seed, and already formed BHs are deposited into larger mass systems due to hierarchical mergers. Our model predicts that at $z = 0$, all haloes above $10^{11}\,M_\odot$ should host a BH (in agreement with observational results), most probably inherited during their lifetime. Haloes less massive than $10^9\,M_\odot$ have a higher probability to host a native BH, but their occupation fraction decreases below 10 per cent.

Key words: black hole physics – hydrodynamics – stars: Population III – galaxies: high-redshift – galaxies: nuclei.

1 INTRODUCTION

Supermassive black holes (BHs) are currently thought to be at the heart of physical mechanisms that shape the galaxy population we observe today. Correlations of their masses with the large-scale properties of their galaxy hosts (Ferrarese & Merritt 2000; Gebhardt et al. 2000; Tremaine et al. 2002; Gültekin et al. 2009) are now accepted as fundamental constrains for every theoretical model trying to explain the evolution of the BH population.

The emergence of supermassive BHs of $10^9\,M_\odot$ already at redshift 6 (Fan et al. 2001, 2004) favours an early formation and rapid growth. Which process allows for the appearance of these seeds is still not well established, nor is the question that what is the characteristic mass of the seeds. A range of possibilities have been explored that belong to the following channels (see Volonteri 2010, for a more comprehensive review):

(i) Population III (PopIII) stars with masses above $260\,M_\odot$ are expected to end their lives leaving a relic BH of comparable mass, because of negligible stellar mass loss (Madau & Rees 2001; Heger et al. 2003; Volonteri, Haardt & Madau 2003; Freese et al. 2008; Iocco 2008; Tanaka & Haiman 2009). This small seed, housed in a growing halo, later grows through accretion and mergers.

(ii) A compact star cluster can be subject to rapid segregation of the most massive stars in its core. If mass segregation occurs before copious mass loss, massive stars decouple dynamically from the rest of the cluster and start colliding in a runaway fashion. The

*E-mail: bernadetta@strw.leidenuniv.nl

mass spectrum evolves in such a way that a single very massive star (VMS) grows quickly (Portegies Zwart et al. 1999; Gurkan, Freitag & Rasio 2004; Freitag et al. 2006a,b). Its growth is terminated once the reservoir of massive stars is exhausted, either via dynamical collisions (as they are all engulfed in the VMS) or via stellar evolution. At low metallicity (below $\approx 10^{-3}$ solar), stellar mass loss is reduced compared to the solar metallicity case (see e.g. Hirschi 2007; Vink 2008; Glebbeek et al. 2009). A sufficiently massive VMS is then expected to end its life leaving behind a remnant BH of a few hundred to a thousand solar masses (Portegies Zwart et al. 2004; Belkus, Van Bever & Vanbeveren 2007; Yungelson et al. 2008).

(iii) Metal-free haloes with virial temperatures above 10^4 K can be suitable sites for gas-dynamical instabilities leading to strong gas inflows in the nucleus of the forming halo. A VMS or a quasi-star can form directly in these nuclei, which collapses in the form of a BH (Haehnelt & Rees 1993; Loeb & Rasio 1994; Eisenstein & Loeb 1995; Bromm & Loeb 2003; Koushiappas, Bullock & Dekel 2004; Begelman, Volonteri & Rees 2006; Spaans & Silk 2006; Lodato & Natarajan 2007; Dijkstra et al. 2008; Natarajan et al. 2009; Spolyar et al. 2008; Volonteri, Lodato & Natarajan 2008; Volonteri & Begelman 2010; Dotan, Rossi & Shaviv 2011). Here, the BH seeds can be as massive as $10^{4-5}\,M_\odot$ (Volonteri 2010).[1]

(iv) BH seeds can ensue as the result of processes arising in the very early universe within a region of space where the gravitational force overcomes pressure (Carr 2003; Khlopov 2010).

In Devecchi et al. (2010, hereafter Paper I) and Devecchi & Volonteri (2009, hereafter DV09) we focused on the second channel. We explored the formation of NCs and BH seeds in dark matter haloes whose gas has been polluted just above a critical metallicity Z_{crit} for fragmentation and ordinary star formation. Gas, initially heated at the virial temperature T_{vir} of the halo, cools down and forms a disc. Gravitationally unstable discs are subject to both mass inflows and episodes of star formation, in both the central and outer parts of the disc. These early central star-forming clusters can provide scaled replica of the nuclear clusters (NCs) we observe today. Our key finding was that these NCs are dense enough to be sites for the onset of runaway collisions, ending with the formation of a BH seed.

In this paper (Paper II) we include the BH population rising from PopIII stars and study their joint evolution. In order to be effective, each of these mechanisms requires specific conditions to be met. The hierarchical build-up of dark matter haloes, together with the evolution of their baryonic component, needs to be followed in detail to constrain the efficiency of the two different BH formation paths. Critical factors that control and regulate this efficiency are the chemical, radiative and mechanical feedbacks from the star-forming haloes. These feedbacks (neglected in Paper I) affect the evolution of the halo gas as they fix the available cooling channels and are then fundamental ingredients if one wants to study the competition between different BH formation paths. We here implement these feedbacks within a semi-analytical model for galaxy formation. This is the first time that this approach is used in the context of BH seed formation.

This paper is organized as follows. In Section 2 we highlight the procedure adopted in describing the evolution of the baryonic component. We include the contribution of both PopIII and PopII/I stars, with their chemical, mechanical and radiative feedback effects. We describe how we populate metal-free haloes with PopIII stars and briefly review the procedure adopted for haloes with $Z > Z_{crit}$ (see

---

[1] It has been speculated that substantial inflows in major mergers can lead to massive BH seeds weighing more than $10^6\,M_\odot$ (Mayer et al. 2010).

Paper I). In Section 3 we present our simulations; and in Section 4 we describe the results. Section 5 contains our conclusions.

2 POPIII FORMATION

Here, we describe our recipe for the evolution of the baryonic component hosted in a dark matter halo of mass M_h, circular velocity V_h, virial radius R_h and spin parameter λ. The behaviour of the gas strongly depends on the available channels for cooling. These in turn rely upon the chemical species available. It has been proposed that a critical metallicity Z_{crit} exists above which fragmentation into PopII/I star formation occurs (Bromm et al. 2001; Omukai et al. 2005; Santoro & Shull 2006; Schneider et al. 2006; Omukai, Schneider & Haiman 2008; Smith et al. 2009; Clark, Glover & Klessen 2008; Safranek-Shrader, Bromm & Milosavljevic 2010). Hence, we distinguish between metal-free haloes (i.e. those systems whose gas still has a pristine composition) and haloes whose gas has been enriched above Z_{crit}. We assume that the formation of PopIII stars sets in only for $Z < Z_{crit}$. Following DV09 and Paper I, we assume a density-dependent Z_{crit}. The relationships adopted in our study are those found by Santoro & Shull (2006). Our reference value for the minimum $Z_{crit} \sim 10^{-5}\,Z_\odot$.

The first stars can form only in those haloes where cooling allows baryons to dissipate energy and condense in the centres of the dark matter potential wells. The first collapsing haloes have virial temperatures smaller than 10^4 K, i.e. the temperature at which cooling from electronic excitation of atomic hydrogen becomes effective.[2] In order for their gas to cool down and form the first stars, minihaloes with $T_{vir} < 10^4$ K must rely on the less effective molecular hydrogen (H_2) cooling.

The critical minimum halo mass $M_{PopIII,crit}$ that is necessary in order for the gas to cool down efficiently and form a PopIII star roughly corresponds to $T_{vir} \gtrsim 10^3$ K (Tegmark et al. 1997). The presence of a UV flux impinging on to the halo increases $M_{PopIII,crit}$. We will briefly discuss this topic in the following section.

If enough H_2 is present, gas can efficiently cool down to $T \sim 200$ K, reaching densities of 10^4 cm^{-3}. We here assume that PopIII stars form in haloes with $T_{vir} \gtrsim 10^3$ K. We estimate the redshift at the formation of the star following Trenti & Stiavelli (2009). After the dark matter halo virializes at redshift z_{vir}, a time-scale of the order of

$$\tau_{form} = 7.6 \times 10^5 \, \text{yr} \left(\frac{M_h}{10^6\,M_\odot}\right)^{-2.627} \left(\frac{1+z_{vir}}{31}\right)^{-6.94}$$
$$+ 8.82 \times 10^6 \, \text{yr} \left(\frac{1+z_{vir}}{31}\right)^{-3/2} \quad (1)$$

is needed for the gas to cool down and collapse.

Yoshida et al. (2003) develop cosmological simulations aimed at studying PopIII star formation in a cosmological context. They show that cooling of the gas can be prevented by dynamical heating of the halo as a result of subsequent mergers. This delays PopIII star formation in fast growing haloes. We calculate the effect of dynamical heating following Yoshida et al. (2003). We halt PopIII formation in those haloes where the dynamical heating rate is higher than the cooling rate.

Despite the large number of studies performed, the initial mass function (IMF) of PopIII stars is still poorly constrained. Simulations of the initial phase of the formation of these object show that

---

[2] In the following we will refer to mini (macro)-haloes as those haloes with virial temperature smaller (greater) than 10^4 K.

massive ($\sim 10^3$ M$_\odot$) clumps of gas can collapse leading to the formation of a very dense, optically thick core of ≈ 0.01 M$_\odot$. Gas in the envelope accretes into the core, increasing the mass of the protostar. The characteristic final mass at the end of the accretion process can be much less than the initial clump mass: feedback effects can strongly reduce the ability of the core to accrete material (see Omukai & Palla 2003; McKee & Tan 2008). In addition, the characteristic mass of the star depends on factors such as the presence of an external UV radiation background, and/or the temperature of the cosmic microwave background floor (see the discussion in Trenti et al. 2009). We assume that a single PopIII star forms in any given halo. The mass of the star is extracted from a distribution function $\Phi(m) \propto m^{-(1+x)}$ with $x = 1.35$, extending from a minimum and maximum masses of 10 and 300 M$_\odot$, respectively (Omukai & Palla 2003; McKee & Tan 2008). Note that recent studies (see Glover et al. 2008; Stacy, Greif & Bromm 2009; Turk, Abel & O'Shea 2009; Prieto et al. 2011) have pointed out that also PopIII stars can form in clusters, where each of star's mass is much lower than the ~ 100 M$_\odot$ predicted by simulations that showed no fragmentation and the formation of a single protostar. In Section 6 we briefly discuss how this could affect our results.

2.1 Radiative feedback

Feedback effects from the first episodes of star formation can strongly modify the efficiency at which gas is able to cool and condense into stars. We here try to obtain a rough estimate of the radiative feedback on PopIII star formation efficiency, postponing the discussion of chemical and mechanical feedback [via supernova (SN) explosions] to the next section.

PopIII stars can produce copious amount of UV photons that can affect the thermodynamics of gas inside the halo and in its neighbours. In particular, photons in the Lyman–Werner (LW) band (11.2–13.6 eV) can photodissociate H$_2$ molecules, thus suppressing cooling below 8000 K. The formation of new zero-metallicity stars is then suppressed (or at least delayed) if the H$_2$ dissociation rate is higher than its formation rate. Self-shielding of the gas in the densest region can prevent H$_2$ disruption by external radiation, this effect being more efficient in the most massive haloes. Machacek, Bryan & Abel (2001) found a minimum threshold halo mass M_{TH} that is necessary in order for PopIII star formation to set in (see also O'Shea & Norman 2008; Trenti et al. 2009; Wolcott-Green, Haiman & Bryan 2011). M_{TH} depends on the LW flux J_{LW} that reaches the halo and can be written as

$$M_{TH}/M_\odot = 1.25 \times 10^5 + 8.7 \times 10^5 J_{LW}^{0.47}, \qquad (2)$$

where J_{LW} is in units of 10^{-21} erg s^{-1} cm^{-2} Hz^{-1}.

For each metal-free collapsing halo, we calculate the total LW flux intercepted by the halo. Radiation sources are haloes hosting an emitting PopIII star and those with ongoing PopII/I star formation (see the next section). We allow the new halo to form a PopIII star only if its mass is above M_{TH}.

Photon luminosities in the LW band are taken from Schaerer (2002) as a function of the star's mass. The effective amount of photons that are able to escape from the PopIII host halo depends on the details of the system. Radiation can be trapped in the dense gas in which the PopIII star is embedded. The escape fraction of photons in the LW band f_{esc}^{LW} depends on the luminosity of the star (and consequently on its mass) and on the potential well of the host. A critical mass of the host that corresponds to $f_{esc}^{LW} \sim 1$ per cent has been calculated (Kitayama et al. 2004, but see also Alvarez, Bromm

& Shapiro 2006; Whalen, Abel & Norman 2004)

$$M_{h,esc}^{LW} = 7.5 \times 10^6 \left(\frac{m_{PopIII}}{200 \, M_\odot} \right)^{3/4} \left(\frac{1 + z_{vir}}{20} \right)^{-3/2} M_\odot. \qquad (3)$$

For haloes with masses $M_h > M_{h,esc}^{LW}$ we assume no LW photons are emitted. On the other hand, we assume $f_{esc}^{LW} = 1$ for $M_h < M_{h,esc}^{LW}$. We adopt this sharp transition motivated by the steep decrease of f_{esc}^{LW} as a function of the host mass as shown in figs 4, 5 and 6 in Kitayama et al. (2004).

2.2 Supernova feedback: metal enrichment and gas stripping

After ≈ 3 Myr massive PopIII stars start to explode in SNe. Metals processed in their centres are released into the halo gas during the explosion and eventually propagate into the intergalactic medium for sufficiently violent bursts. SN explosions in high-redshift haloes can be extremely destructive. SNe-driven bubbles can push away part of the gas in the halo, eventually fully depriving the host of its gas.

Metal yields and burst energies can strongly differ depending on the mass of the progenitor star. The evolution of PopIII stars has been studied in details by Heger & Woosley (2002). They found that stars with masses below 40 M$_\odot$ explode as SNe, releasing part of the metals they produce. Stars with masses between 140 and 260 M$_\odot$ are expected to be completely disrupted in pair instability SNe. Stars with masses between 40 and 140 M$_\odot$ and above 260 M$_\odot$ instead are expected to lead to direct BH formation with a mass comparable to that of the progenitor star. For these two ranges of mass we assume no metals are ejected. Each time a PopIII star explodes, a fraction of its initial mass is converted into metals. Metal yields are taken from Heger & Woosley (2002). We assume the ejected metals efficiently mix with the gas of the halo. The new metallicity of the halo gas is calculated by taking into account the total amount of metals released, plus those already in place.

Explosion energy, E_{SN}, of a PopIII star depends on its mass, and its value ranges between 10^{51} and 10^{53} erg (see fig. 1 in Heger & Woosley 2002). Values of E_{SN} as high as 10^{53} erg can easily evacuate a large fraction (up to 95 per cent) of the gas initially present in the host (Whalen et al. 2008). The efficiency of gas depletion depends on the depth of the potential well of the host and on the ability of the star to photoionize and photoevaporate the gas. Mini-haloes can be disrupted even by PopIII progenitors of 15 M$_\odot$ while more massive systems are much more resistant. In order to fix the amount of gas that remains in a halo, we here adopt the same treatment as in Paper I. We calculate the amount of energy channelled into the outflow and assume the shell to evolve following the Sedov–Taylor solution. This allows us to infer the energy of the outflow, K_{sh}, and its mass, M_{sh}, at the moment it reaches the virial radius. M_{sh} can be calculated by comparing K_{sh} with the change in binding energy before and after the explosion and it equals:

$$M_{sh} = \frac{f_w E_{SN}}{2 \, (1 + \Omega_b/\Omega_m) \, G M_h/R_h + (1/2) v_{sh}^2}, \qquad (4)$$

where f_w is the fraction of the released energy channelled into the outflow (for the exact expression of f_w see Paper I and Scannapieco, Schneider & Ferrara 2003) and v_{sh} the velocity of the shell at R_h (see appendix A of Paper I for the details of the calculation). This corresponds to a retention fraction, $f_{ret} \equiv (M_{gas} - M_{sh})/M_{gas}$. After the explosion we assume that a fraction $(1 - f_{ret})$ of the metal yields produced in the PopIII star propagates into the medium surrounding the halo.

3 POPII-I STAR FORMATION: THE LOW-MASS MODE

A single PopIII star explosion can easily pollute its host above the critical metallicity for fragmentation Z_{crit}. Polluted gas that cools down settles in a disc, and can start forming stars in the low-mass mode. For the mass distribution of this stellar population we adopt a Salpeter IMF, in the mass range 0.1–$100 \, M_{\odot}$. Gravitational instabilities in these discs can also lead to mass inflow and nuclear star formation so that an NC can form. Rapid dynamical evolution in the cluster core may eventually lead to the formation of a BH seed. This model for BH seed formation has been discussed in details in Paper I and in DV09. We here briefly review key points of the model.

(1) Hot halo gas in virial equilibrium cools down at a rate $\dot{M}_{cool}$ computed according to the available cooling channel (either molecular or atomic cooling; see Paper I) and forms a disc. The disc follows a Mestel profile and we calculate its structural parameters as described in Paper I.

(2) As gas cools down, the disc mass increases. The disc is unstable if its Toomre parameter Q (Toomre 1964) decreases below a critical threshold Q_c. Below Q_c the disc develops non-axisymmetric structures, leading to inflows and star formation. Inflows, at a rate

$$\dot{M}_{grav} = \eta \left(\frac{Q_c^2}{Q^2} - 1 \right) \frac{c_s^3}{\pi G}, \tag{5}$$

cause a redistribution of the disc mass that is transported into the nuclear region. Here c_s is the sound speed of the gas, $\Sigma(R)$ its surface density profile and η the inflow efficiency. A steeper profile develops in the inner part of the disc within a transition radius R_{tr}.

(3) Stars form inside a star formation radius R_{SF}. This is calculated as that radius at which the adiabatic heating rate of the gas equals its cooling rate. We assume that the star formation rate follows a Kennicutt–Schmidt relation (Schmidt 1959; Kennicutt 1998). The star formation rate $\dot{M}_{*,d}$ in the Mestel disc scales with the disc parameters as $\propto (\Sigma_0 R_0)^{7/5} (R_{SF}^{3/5} - R_{tr}^{3/5})$. Star formation induces a reduction of the available gaseous mass that can be transported in the nucleus. The net inflow rate is $\dot{M}_{inf} = \dot{M}_{grav} - \dot{M}_{*,d}$.

(4) Mass accumulated into the nucleus forms a compact cluster of stars. We calculate the core collapse time-scale t_{cc} of the clusters and select those clusters with $t_{cc} < 3 \, Myr$, i.e. systems in which the dynamical evolution precedes stellar evolution. We follow the formalism of Portegies Zwart & McMillan (2002) to infer the mass M_{VMS} of the VMS as a function of the cluster parameters. We select as possible sites for BH seed formation only low-metallicity clusters, i.e. systems with $Z < 10^{-3} \, Z_{\odot}$, as at higher metallicity the star loses mass in winds and the final BH remnant has low mass (at most a few tens solar masses). Each time $Z < 10^{-3} \, Z_{\odot}$ and $M_{VMS} > 260 \, M_{\odot}$, i.e. it surpasses the threshold for pair instability SNe, a BH forms.

We also consider the contribution of PopII stars as sources of LW photons. The LW luminosity associated with a star formation rate $\dot{M}_*$ is calculated as $L_{LW} = 8 \times 10^{27} \dot{M}_* \, erg \, s^{-1} \, Hz^{-1}$ (Dijkstra et al. 2008). This luminosity is associated with every halo that is forming PopII stars, given its $\dot{M}_*$. This information is used to compute the LW flux impinging on surrounding haloes when we determine whether H_2 is photodissociated or not (see e.g. equation 2).

SN explosions from evolved stars can lead to strong gas depletion, particularly in the shallowest potential wells. We calculate the mass-loss rate from the halo $\dot{M}_{sh}$ resulting from multiple explosion, as

$$\dot{M}_{sh} = \frac{f_w \nu_{SN} E_{SN} \dot{M}_*}{2 \left(1 + \Omega_b / \Omega_m \right) G M_h / R_h + (1/2) v_{sh}^2}, \tag{6}$$

where f_w is the fraction of energy channelled into the outflow, $\nu_{SN} = 0.004\,84$ is the number of SNe exploding after the formation of a mass in star M_* divided by M_*, $E_{SN} = 10^{51} \, erg$ is the energy of a single explosion and v_{sh} is the velocity of the outflow at the virial radius (see Paper I for details).

4 SIMULATIONS

Simulations are run in two steps. We first build up the dark matter merger history, and then populate this skeleton with galaxies, including all the baryonic processes described in the previous sections.

We keep track of the evolution of the dark matter component running simulations with the code PINOCCHIO (Monaco et al. 2002a; Monaco, Theuns & Taffoni 2002b). PINOCCHIO initializes a density perturbation field on a 3D grid. The density field is evolved via the Lagrangian Perturbation Theory in order to generate catalogues of properties (like mass, position and velocity) and merger history of each virialized halo.

We consider cosmological volumes of 5 and 10 Mpc (comoving) length. We adopt a Λcold dark matter (ΛCDM) cosmology with $\Omega_b = 0.041$, $\Omega_m = 0.258$, $\Omega_{\lambda} = 0.742$, $h = 0.742$ and $n_s = 0.963$, as given by five-year *Wilkinson Microwave Anisotropy Probe* (*WMAP*) data (Dunkley et al. 2009). Dark matter merger trees are followed up to $z = 0$.

We follow the evolution of the baryonic component by applying the prescriptions described in Paper I and in the previous section. We halt our simulations at redshift 6. After this redshift the BH formation rate decreases, indicating that the bulk of the BH seed population has already formed (see the following sections).

Fig. 1 illustrates the recipes adopted in our semi-analytical model. At first all haloes are metal free with a baryonic gas fraction equal to Ω_b / Ω_m. In each redshift interval and for each halo, we apply the prescriptions described in Sections 2 and 3. The evolution of each halo then depends not only on the merger history of its dark matter component, but also on the earlier history of its baryonic component. This is traced self-consistently starting from the first PopIII star formation episode. For each halo, we evaluate if and when a PopIII star forms. The star can either end forming a BH seed or it can release metals: metal enrichment starts as soon as haloes are polluted by these first metals. Enriched gas starts cooling again, at a rate depending on the amount of metals and gas that the host is able to retain.

Spatial positions are stored from the PINOCCHIO output with steps in redshift of 0.25 (corresponding to 1–2 Myr at $z \sim 20$ and 10–20 Myr at $z \sim 6$–10). This information is used in our semi-analytical model in order to calculate radiative feedback from/on haloes when the emitting sources are active. Every time halo positions are updated we also examine which sources are active. Such fine time resolution is required to estimate the effect of radiative feedback and the production of LW photons, especially in the case of PopIII stars. Since the UV emission is limited to a few million years, the short lifetime of these massive stars, the effect depends on the duration of the emission and on the collapse time of haloes surrounding each halo hosting PopIII stars. If the time resolution is too coarse, radiative feedback is not correctly evaluated. This is a consequence of the short active time of some sources, particularly PopIII stars; if their activity is not monitored with a high enough time frequency,
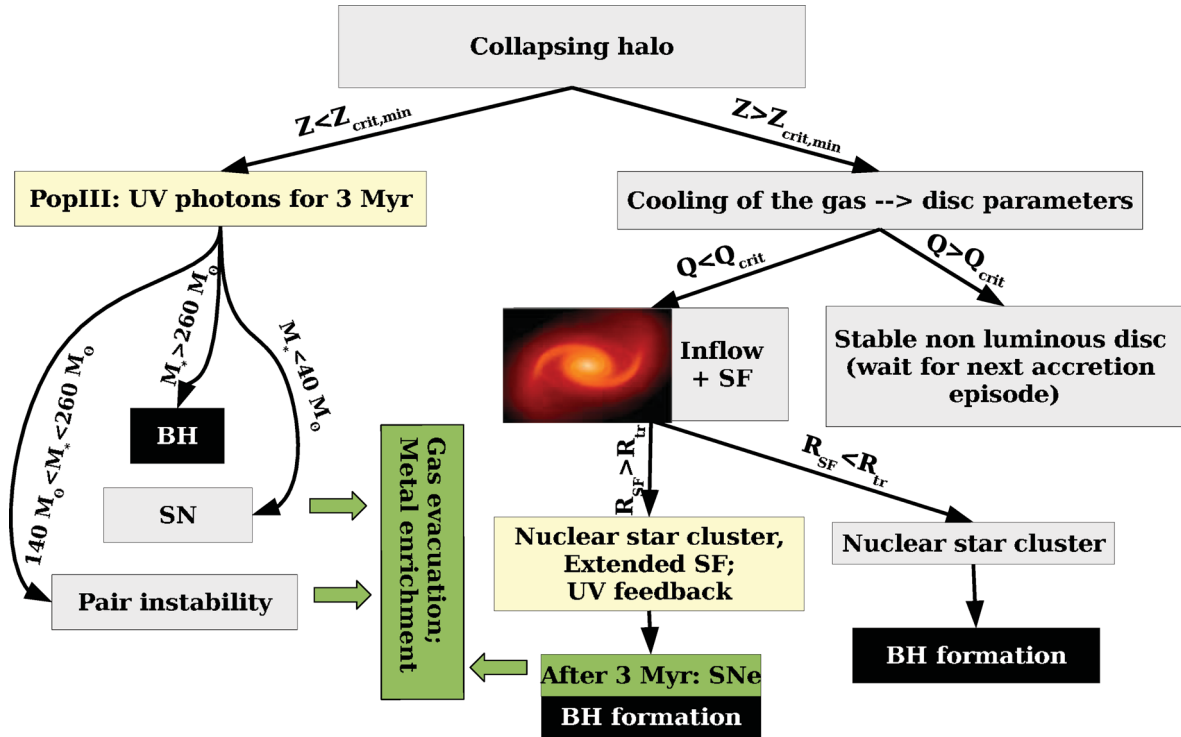
Figure 1. Flow chart of the model (outlined in Section 2) illustrating the different pathways that terminate with the formation of a seed BH, and the different prescriptions used to model the dissipative behaviour of the baryonic component. Dark grey areas (green areas in the online version of this manuscript) correspond to those parts of the code associated with supernova feedback. Light grey boxes (yellow areas in the online version of this manuscript) correspond to those parts of the code associated with radiative feedback. Black boxes indicate the presence of a channel for the possible formation of a BH seed (either as remnant of a PopIII star or as a result of dynamical instabilities in a newly formed nuclear stellar cluster).

the LW flux is initially underestimated. When this happens more haloes are allowed to form stars. This burst of star formation increases the level of LW flux acting on the next redshift interval, so that in this new time-step the amount of stars (and consequently LW photons) that form abruptly decreases. At $z > 20$ when star formation is dominated by PopIII stars, our time-steps are shorter than the lifetime of these objects. This guarantees that we can correctly account for the presence of the emitting sources, and estimate the LW flux adequately.

In the current cosmological scenario, merger events are quite frequent in the history of dark matter haloes. Every time two dark matter haloes merge we adopt the following prescriptions: we assume that the newly formed halo has total, baryonic, stellar and metal masses given by the sum of the progenitor ones. For the mass ratio less than 1/10, we assume the spin parameter of the main progenitor to be retained, otherwise a new spin parameter is generated (according to the spin distribution found in cosmological simulations; Bett et al. 2007). The properties of the new baryonic disc are then calculated taking into account its new mass and angular momentum. Its stability is evaluated and eventually an episode of inflow and star formation sets in. Note that in this way, star formation events are calculated taking into account only the stability of the structure at the end of the merger and not the tidal torques acting during the event. The metallicity of the gas merger remnant is calculated adding together the amount of metals of the two merging systems. Also in this case we assume efficient mixing.

In some cases one or both merging haloes host a BH. Our simulations are not able to follow the detailed evolution of the merging process and to assess if the BH hosted in the secondary galaxy is able to reach the centre of the primary. Our prescription only relies

on the mass ratio between the two galaxies. For merging systems with mass ratio greater than 1/10, we assume the secondary BH to reach the centre of the merger remnant (Callegari et al. 2009). If both galaxies originally hosted a BH, the two are assumed to merge. Below the 1/10 halo mass ratio the secondary BH (if present) is left wandering in the new halo.

Our technique represents an optimal compromise between cosmological simulations and standard semi-analytical codes. Our merger trees contain the spatial and kinematical information on dark matter haloes, allowing us to determine the effects of feedback and metal pollution on neighbouring haloes, and taking into account mergers and dynamical interactions. By using our semi-analytical model we can study gas evolution and its impact on BH evolution at arbitrary resolution, which is not possible even in the highest resolution cosmological simulations (e.g. Sijacki, Springel & Haehnelt 2009; Bellovary et al. 2011).

5 BLACK HOLE SEED FORMATION

5.1 Properties of the BH population

We here discuss a model in which we adopt a PopIII IMF in the range 10–300 $M_\odot$, an inflow efficiency $\eta = 0.3$ and $Q_c = 2$. The $Z_{crit} - n_{crit}$ prescription adopted here is the same as in Paper I, giving a minimum $Z_{crit} \sim 10^{-5} Z_\odot$.

Fig. 2 shows the fraction of virialized haloes that form a seed BH, at a given redshift, either via the dynamical (dashed line) or via PopIII (solid line) channel. The thin solid line represents our resolution limit on the number of halo (i.e. it is one over the total number of haloes at that z). As already found in previous studies
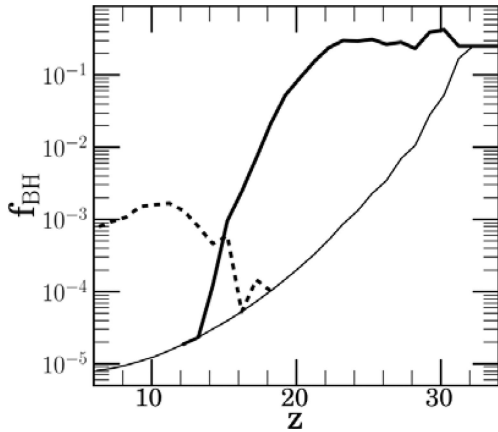
Figure 2. Fraction of haloes f_{BH} that at a given redshift z are forming a BH seed in situ, either from the PopIII (solid line) channel and from the dynamical (dashed line) channel. The thin solid line represents the resolution limit of the simulation with respect to the number of haloes.

BHs, remnants of PopIII stars, start forming early on ($z \sim 30$; Yoshida et al. 2003; Ciardi & Ferrara 2005; Maio et al. 2010, Maio et al. 2011). They become increasingly rarer with cosmic time as a result of chemical and radiative feedback.[3] In our simulations their formation stops around $z \sim 10$–15. BHs from stellar instabilities in NCs form early after the death of the first PopIII stars. They initially are rare events: suitable haloes are only a sub-sample of those systems that previously hosted a PopIII star. With time, metal enrichment spreads out in a larger number of systems. The fraction of haloes that form a seed BH, at a given redshift, via the dynamical channel grows between redshift 20 and 10 from $f_{BH} \sim 10^{-4}$ to $f_{BH} \sim 0.002$ and then declines. Note that the two BH formation channels considered in this paper overlap in time only for a brief epoch.

Fig. 3 (upper panel) shows the mass function of seeds formed at $z > 6$ through the dynamical channel alone. M_{BH} spreads in the range 300–3000 $M_{\odot}$. Most BHs have masses around a few hundred $M_{\odot}$, with a tail that extends up to 3000 $M_{\odot}$. Fig. 3 (lower panel) shows mean BH seed masses $\langle M_{BH} \rangle$ versus redshift. $\langle M_{BH} \rangle$ goes from 300 $M_{\odot}$ at $z \sim 15$–20 to $10^3 M_{\odot}$ at $z = 6$. Heavier BH seeds form at lower redshift when haloes become increasingly heavier, retaining more gas after PopIII explosions. In these deeper potential wells, unstable discs build up more easily due to the higher gas content. Stronger inflows can develop due to the higher gas densities, thus allowing for higher M_{BH}.

Fig. 4 shows comoving mass densities of seeds, ρ_{seed}, in our reference model. The dashed (dotted) line corresponds to the PopIII (dynamical) channel, and the solid line corresponds to the total seed mass density. The PopIII channel dominates ρ_{seed} at early time, from redshift $z \sim 30$ down to $z \sim 15$. The dynamical channel becomes important at later times ($z \sim 13$) due to the increasing effects of the radiative and chemical feedbacks. The density, ρ_{seed}, continues to increase up to the minimum redshift of the simulation ($z = 6$). The lower number of PopIII stars that can form (and consequently the lower number of relic BHs) at $z \lesssim 20$ causes the flattening of ρ_{seed}

---

[3] Note, however, that in a study by Bellovary et al. (2011), a second peak of BH formation is found at later times. They notice that this could be due to the presence of metal enrichment inhomogeneity within larger haloes. Pockets of still metal-free gas clouds within the larger haloes can provide suitable sites for PopIII formation. This effect is not visible in our simulation due to the assumption of efficient mixing of metals within a single halo.
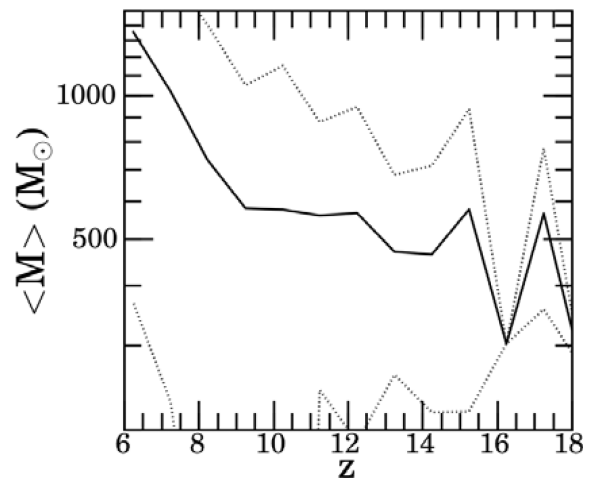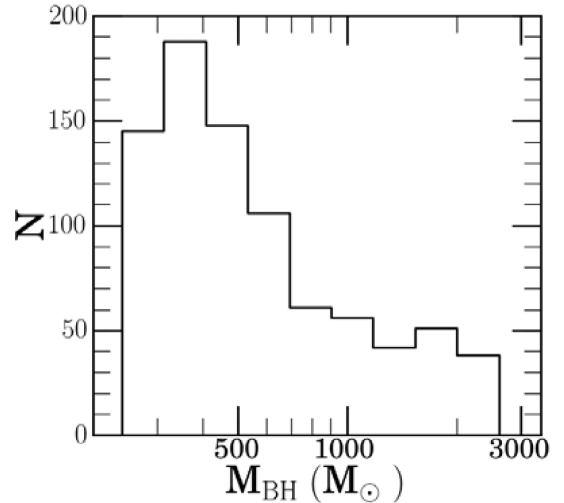

Figure 3. Top panel: mass function of seed BHs formed via stellar dynamics in NCs, for our reference model. Bottom panel: mean mass as a function of redshift z for the same formation channel. Dotted lines denote the dispersion at 1σ level.

around $z \sim 20$, which is followed by the rising contribution of the dynamical channel.

5.2 Where do BHs form and reside?

In order for a BH seed to form, specific conditions need to be fulfilled in the housing halo. These were discussed in Sections 2 and 3. Once formed, BHs are implanted and redistributed inside haloes via mergers. The population of BH-hosting haloes is therefore shaped both by the formation mechanisms and by the hierarchical merging process. To which extent each of these two phenomena is more relevant depends on both halo properties and redshift.

In the local Universe, BHs are known to reside in the most massive galaxies, their occupation fraction being equal to 1 for the most massive systems. Fig. 5 (panel a) shows the fraction F_{BH} of haloes hosting a BH at $z = 20, 15, 10, 6$ (curves from left to right) as a function of the halo mass M_h. The occupation fraction increases with increasing M_h in a self-similar way: as redshift decreases the shape of $F_{BH}(M_h)$ remains the same, but shifts towards larger masses. Above a characteristic mass (that depends on z) $F_{BH} = 1$. This shift is due to two effects: (i) as redshift decreases, smaller mass
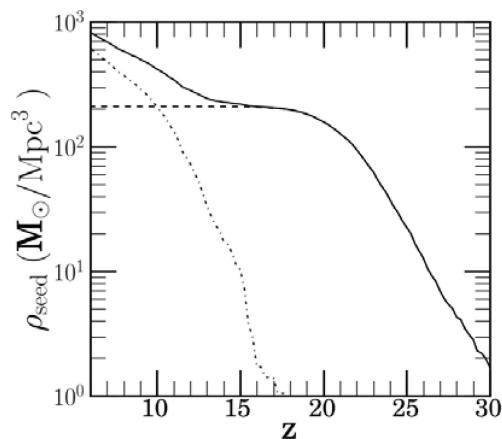
Figure 4. Comoving seed densities versus redshift z. Solid line: total comoving BH seed density. Dashed line: $\rho_{\rm seed}$ versus z for BH seeds formed as relics of PopIII stars more massive than $260\,{\rm M}_\odot$. Dotted line: $\rho_{\rm seed}$ as a function of z, for BHs formed via dynamical instabilities in NCs.

haloes are progressively less effective in forming a BH seed: smaller mass systems are more susceptible to feedback effects that become progressively more important as redshift decreases; (ii) haloes that contain BHs merge with others, shifting their mass towards the higher mass range.

Fig. 5 (panel b) shows $F_{\rm BH}$ as a function of the halo mass growth rate ${\rm d}M_{\rm h}/{\rm d}t$. Here ${\rm d}M_{\rm h}/{\rm d}t$ is the mean value calculated along all halo lifetime. Solid, dotted, dashed and dot–dashed lines correspond to $z = 20, 15, 10$ and 6, respectively. BHs reside in those faster growing systems that are also the more massive. This population of hosts evolve in time, reaching higher masses and thus ${\rm d}M_{\rm h}/{\rm d}t$; $F_{\rm BH}$ shifts accordingly maintaining the same shape.

The latter panel in Fig. 5 (panel c) shows $F_{\rm BH}$ as a function of halo density again at $z = 20, 15, 10$ and 6 (solid, dotted, dashed and dot–dashed lines, respectively). With halo density, $\rho_{\rm h}$, we here refer to the environmental density of the surrounding haloes. We use a mass-weighted indicator that accounts for the number and mass of the neighbouring haloes. To calculate $\rho_{\rm h}$ we follow the following procedure: we first identify the sphere centred on the halo that contains its closest 32 neighbours. We then calculate the dark matter density within that sphere and assign this value as $\rho_{\rm h}$. In this case no self-similar trend is found in the behaviour of $F_{\rm BH}$. The probability of hosting a BH is higher for haloes residing in denser environments. This is consistent with the fact that the more massive haloes usually reside in a crowded environment, where they can also grow faster. With decreasing redshift this effect becomes progressively more relevant and $F_{\rm BH}$ steepens considerably for high $\rho_{\rm h}$.

A halo can host a BH either because the BH formed there as *native* BH or because it was deposited after a merger with a secondary system (*inherited* BH). Fig. 6 shows the ratio between the number of inherited ($N_{\rm i}$) and native ($N_{\rm n}$) BHs as a function of z. Solid lines correspond to $N_{\rm i}/N_{\rm n}$ computed for all haloes. $N_{\rm i}/N_{\rm n}$ depends on $M_{\rm h}$, ${\rm d}M_{\rm h}/{\rm d}t$ and z. In order to capture this dependency, we compute this ratio selecting haloes in different mass bins. Different trends can be inferred.

(i) The number of native BHs versus z is a double peaked function, reflecting the different formation efficiency with z of the two formation mechanisms considered here. The number of inherited BHs increases with decreasing z. The ratio $N_{\rm i}/N_{\rm n}$ initially increases, and reaches unity around $z \sim 15$–20 (solid line). At higher z mergers
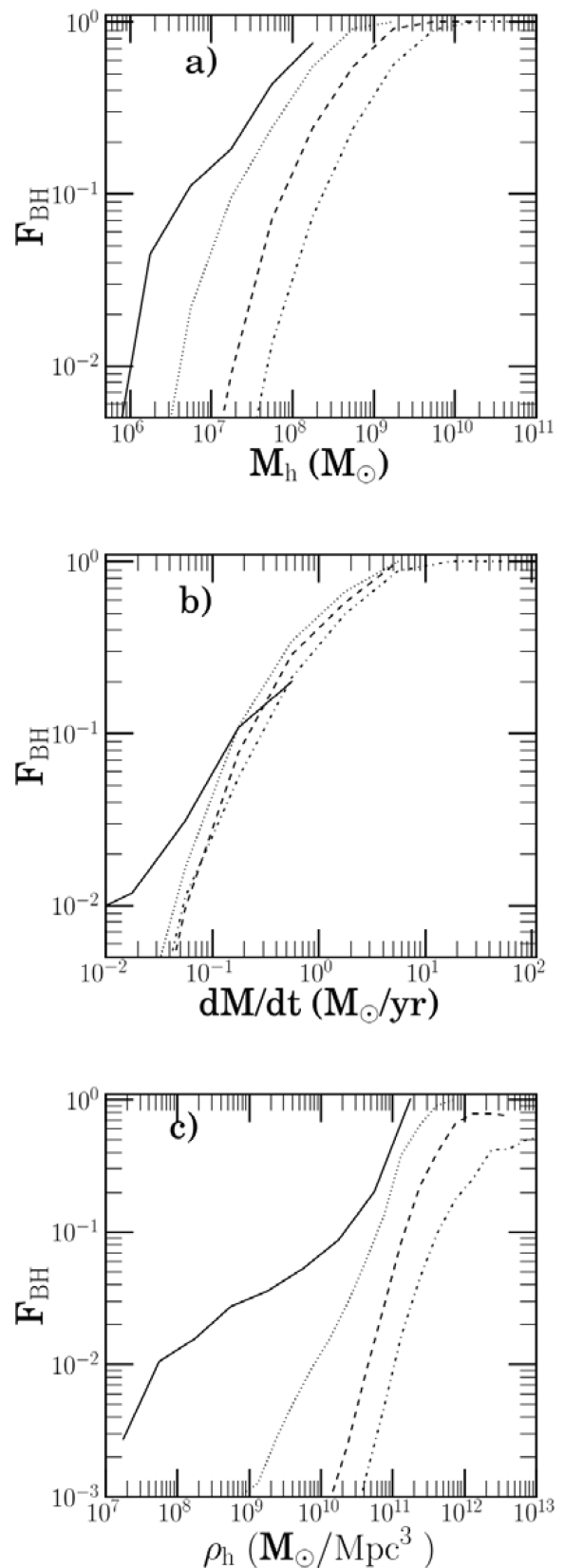
Figure 5. Occupation fraction of BHs as a function of halo masses $M_{\rm h}$ (panel a), growth rate (panel b) and surrounding halo density (panel c). Solid, dotted, dashed and dot–dashed lines correspond to $z = 25, 20, 15$ and 10, respectively.
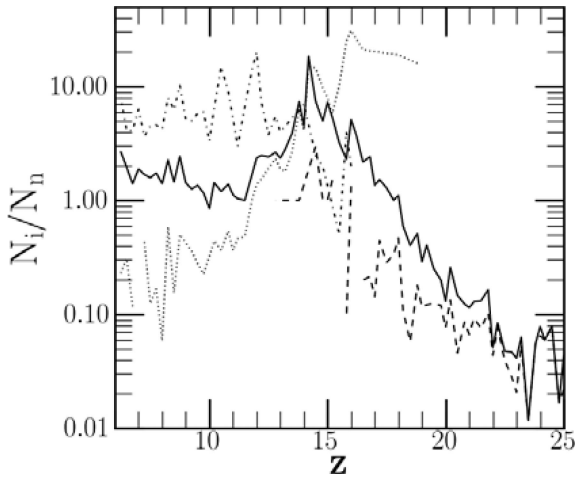
Figure 6. Ratio of the number of inherited (N_i) and native (N_n) BHs versus redshift. The solid line corresponds to N_i/N_n calculated for the all halo population. Dashed, dotted and dot–dashed lines correspond to N_i/N_n calculated including only haloes with $M_h < 10^7 M_\odot$, $10^7 M_\odot < M_h < 10^8 M_\odot$ and $M_h > 10^8 M_\odot$, respectively.

do not have time enough to distribute BHs in sites different from their original formation place: only haloes that form a BH host one. In this regime F_{BH} reflects the efficiency of the formation process. At lower z, conversely, F_{BH} is dominated by the ability of haloes to acquire and implant an already existing BH. We therefore confirm the result originally found by Menou, Haiman & Narayanan (2001, see also Volonteri et al. 2003). N_i/N_n decreases again during the second peak of BH formation (via the dynamical channel) but always remains higher than one.

(ii) Lower mass haloes (the dashed line in Fig. 6) have a high probability of hosting a native BH. In contrast, higher mass haloes (dot–dashed line) more commonly acquire their BHs via mergers. The characteristic mass at which this transition appears shifts towards higher M_h with decreasing z. This causes haloes in the mass range 10^7–$10^8 M_\odot$ (dotted line) to have $N_i/N_n > 1$ at higher z ($\gtrsim 12$), and $N_i/N_n < 1$ afterwards.

(iii) At a given redshift, haloes with higher dM_h/dt more often acquire their central BHs through mergers. The transition between the two regimes is around $dM_h/dt \sim 1$–$2 M_\odot$ yr^{-1}, almost independent of z.

One potential caveat on the discussion above is related to the possibility that the central BH is ejected from its host after a merger with a secondary BH. Anisotropic gravitational wave emission can impart to the remnant high recoil speeds (Baker et al. 2007; Campanelli et al. 2007; González et al. 2007; Herrmann et al. 2007; Koppitz et al. 2007; Schnittman & Buonanno 2007). The strength of the recoil depends on the mass ratio of the two BHs and on their spin orientation. In our simulations we do not follow accretion on to BHs, so we do not have information about mass ratio and spin orientation of the merging components. To estimate, at least at the first order, how ejections can deplete the BH population, we used BH merger histories extracted from our outputs. We impart a kick velocity at each merging binary, at the time of merger, according to the following scheme. We assume BHs are ejected when the kick velocity is larger than the virial velocity of the host halo. We assume a flat distribution of spin magnitudes and randomly oriented BH spins. We adopt this configuration as a potential upper limit to the effect of recoils (Volonteri, Gültekin & Dotti 2010), which could potentially lead to the largest changes in our results. We adopt three

different prescriptions to calculate the mass ratio of the merging BHs in a binary:

(i) we keep the mass of the seed BHs without considering any accretion;

(ii) we consider $M_{BH} = M_{inf}$, i.e. the case in which all the mass channelled in the centre of the halo is accreted into the BH;

(iii) we assume a simple scaling relation to hold between M_{BH} and M_h so that the BH mass ratio is equal to the mass ratio of their host haloes. This prescription is inspired by the M_{BH}–M_{bulge} correlation (Magorrian et al. 1998; Häring & Rix 2004).

In all three cases the fraction of haloes that host BHs changes only by less than 15 per cent at $z = 6$ (for similar studies on the effect of ejections on BH occupation fraction, see also Volonteri et al. 2010; Schnittman 2007). Note that this is an upper limit to the actual efficiency of ejection since in the systems considered in this paper, we would expect the merger to happen in an environment where the two BHs accrete gas from a gas reservoir that has a net angular momentum. The spins of the two BHs are then expected to align with the angular momentum of the binary (Bardeen & Petterson 1975; Perego et al. 2009; Dotti et al. 2010), leading, typically, to lower recoil velocities.

BHs arising from the dynamical channel are expected to form more easily in gas-rich structures with high inflows. In these objects, global star formation is easily activated. As a consequence, we expect the formation of BH seeds through the dynamical channel to be related to the star formation rate in galaxies. Fig. 7 shows the total BH formation rate versus the star formation rate in our simulated cosmological volume for the two channels. Different points correspond to different simulation snapshots, taken at an interval of redshift 0.1. The star formation rate increases with cosmic times. From Fig. 7, it appears that our model predicts a correlation between the global star formation rate and the formation rate of BHs only for the dynamical channel and up to $0.1 M_\odot$ yr^{-1} Mpc^{-3}. At higher star formation rates the correlation changes sign. This is due to the effect of metal enrichment that increases the typical metal content in haloes. At first this increases the number of haloes whose gas
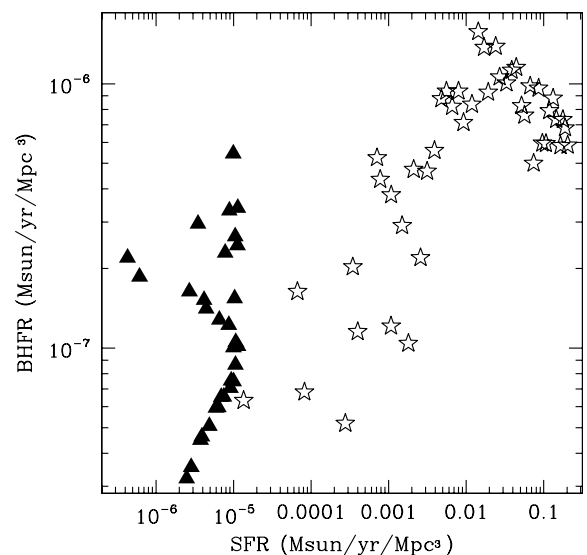
Figure 7. Black hole formation rates versus star formation in our cosmological volume. Triangles refer to PopIII channel while stars refer to the dynamical channel. Points correspond to snapshots of our simulation taken at a different redshift. The z interval considered spans between 10 and 40.

has metallicity $Z_{crit} < Z < 10^{-3} Z_{\odot}$. As more metals are released, the typical Z of haloes suitable for hosting a runaway collision in their centre increases above our threshold for BH formation. BH formation models that require metal-free gas do not produce this correlation (see Bellovary et al. 2011).

5.3 Changing model parameters

We here discuss how our results are affected by changing model parameters, specifically how our results depend on Q_c, η, Z_{crit} and the PopIII IMF. We change each parameter at a time, fixing all the others. Simulations are run with $Q_c = 1$, $\eta = 1$, PopIII masses between 1–300 $M_{\odot}$ and 10–600 $M_{\odot}$. We adopt the different Z_{crit}–n_{crit} relationship discussed in DV09. As a reference, minimum values of Z_{crit} considered are $10^{-6} Z_{\odot}$ and $10^{-4} Z_{\odot}$. We run simulations up to $z = 10$ and compare their results with our reference model at that same z.

A general result of these simulations is that $\langle M_{BH} \rangle$ does not depend strongly upon the model parameters ranging between 600 and 800 $M_{\odot}$ in all our simulations. The main effect that changing model parameters have is on the number of BHs formed. This consequently affects ρ_{seed}.

(i) *PopIII masses:* increasing the maximum mass of PopIIIs does not affect our results. Allowing for a lower minimum mass increases considerably the number of low-mass stars, given our chosen IMF. Metals released by these stars are usually not enough to lead to a strong imprint on their host haloes. The number of haloes where $Z > Z_{crit}$ decreases. This decreases the number of haloes suitable to form BH seeds via the dynamical channel, decreasing ρ_{seed} by a factor of 2–3. Note that we fix the shape of the IMF. A shallower slope would produce a higher fraction of high-mass stars. These would initially produce a higher number of remnant BHs. At the same time the more frequent events of pair instability SNe and larger number of LW photons would suppress PopIII formation earlier than in our models. The formation of BHs in NCs would also start earlier, as the number of haloes with $Z > Z_{crit}$ is increased.

(ii) Z_{crit}: increasing Z_{crit} of 1 order of magnitude decreases the metallicity range within which we allow BHs to form via runaway collisions. This reduces the resulting number of BH formed via this channel by a factor of ~ 30. At the other end, decreasing Z_{crit} of a factor of 10 only increases the number of BH of less than a factor of ~ 2. A single-pair instability SN typically increases the halo metallicity above $10^{-5} Z_{\odot}$, so that only a few haloes have a metallicity between 10^{-6} and $10^{-5} Z_{\odot}$.

(iii) η: higher η allows for faster inflows and the mass of the NCs at the moment of BH formation is consequently higher. A population of NCs not massive enough to build up a VMS of $m_{VMS} > 260 M_{\odot}$ exists in our reference model. For higher η these systems shift towards larger masses. This increases the number of BH formed by a factor of 2.

(iv) Q_c: for $Q_c = 1$ only those haloes hosting the most unstable discs are still prone to instability. These are the same systems in which larger inflows develop. The resulting NC system shows a depletion in its lower mass population and thus a reduction in the number of BHs, particularly at lower masses. This depletion lowers ρ_{seed} by a factor of 2.

6 DISCUSSION

We developed a model for BH seed formation either as remnants of PopIII stars or as a result of runaway stellar collisions in high-

redshift NCs. We devised a scheme for the evolution of the baryonic component, illustrated in Fig. 1. Haloes with $Z < Z_{crit}$ form single PopIII stars, and stars more massive than 260 $M_{\odot}$ provide for a remnant BH of comparable mass, after 3 Myr from formation. PopIII stars are the first sources of radiative, chemical and mechanical feedbacks that affect further evolution of the gas in dark matter haloes. Once haloes are polluted above Z_{crit} we assume that PopII/I star formation sets in. Gas settles down in a disc structure of given mass and angular momentum. Inflows and star formation compete in driving the evolution of the discs that may become unstable. Metal-poor NCs (with $Z_{crit} < Z < 10^{-3} Z_{\odot}$) formed in the central region of the disc can provide suitable sites for runaway collisions, leading to the formation of a VMS and thus of a seed BH.

We explored the properties of the population of evolving haloes, combining the clustering of dark matter haloes (followed with PINOC-CHIO), with our semi-analytical model. Our aim was that of comparing the efficiency of the two mechanisms, PopIII remnants versus dynamical collisions, in shaping the BH seed population.

PopIII stars form BH seeds already at redshift $z \sim 30$, and this is in agreement with previous results. Their rate of formation decreases with decreasing redshift and this channel becomes sterile after $z \sim 15$–20 due to the metal diffusion caused by SN explosions and H_2 dissociation due to LW photons. BH seeds from the dynamical channel start forming early after the rising of the first PopIII. This is due to the rapid pollution that can develop in a halo where a PopIII exploded. But only at later times (i.e. around $z \lesssim 15$), the dynamical channel provides an efficient mechanism for the formation of a larger number of seeds. In addition, masses for seed BHs from the dynamical channel can reach values up to $\sim 10^3 M_{\odot}$ and are typically higher than those left behind by PopIII stars (200 $M_{\odot}$). These two facts both contribute in a rapid increase of seed mass comoving densities. The comoving mass density from runaway collisions exceeds that of PopIII remnants below redshift $z \lesssim 13$.

The BH occupation fraction is sensitive to the halo mass, growth rate and density along the redshift interval spanned in our simulation. BHs reside in higher mass, faster growing systems, that inhabit over-dense regions of the universe. Haloes with these characteristics are more suitable for the formation of native BHs, and/or have higher probabilities to inherit a BH via a merger with smaller systems.

Observations of galaxies at $z = 0$ indicate that the occupation fraction in systems more massive than $\sim 10^{11} M_{\odot}$ is unity (Decarli et al. 2007; Gallo et al. 2008). To check that this is the case also in our model, we analyse the merger tree histories of subsets of our haloes up to $z = 0$. Haloes above $10^{11} M_{\odot}$ all host a BH, most probably inherited already before $z = 6$. Our predicted F_{BH} at $z = 0$ drops below 10 per cent at $M_h \sim 10^9 M_{\odot}$. Below this mass BHs are very rare, and when present they have a probability higher than 50 per cent of being native BHs.

In our model, we assumed that PopIII stars form as single objects in any given halo. Recent studies, however, have shown that even metal-free gas can fragment into multiple clumps, possibly leading to the formation of a PopIII stellar cluster (Stacy et al. 2009; Turk et al. 2009; Clark et al. 2011; Prieto et al. 2011). This fragmentation process can lead to lower PopIII star masses, eventually precluding the formation of objects with masses higher than 260 $M_{\odot}$. This could in principle inhibit the formation of BH seeds via this channel. We note, however, that PopIII proto-clusters form as high-density systems (Clark et al.) where collisions between stars could still lead to the formation of a VMS (Devecchi et al., in preparation).

In this paper we ignore the BH growth due to the accretion of gas as we do not take into account the competition of BHs and NCs in
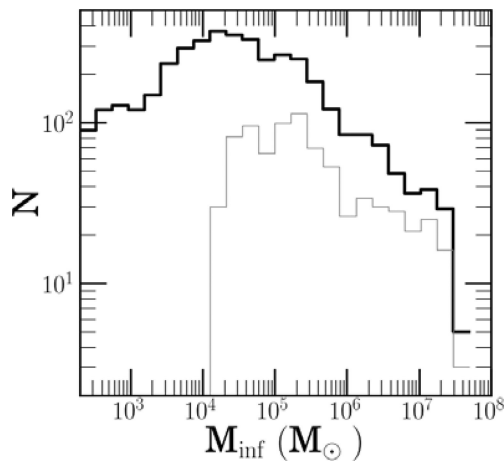
Figure 8. The distribution of mass M_{inf} inflowing at the centre of haloes, accumulated until redshift $z = 6$ (solid line). The thin solid line corresponds to those systems that host a BH in their centre, and this represents an upper limit to the BH mass.

sharing inflowing gas after their formation. We can infer safe upper limits for the BH or NC masses investigating the amount of gas that flows into the nucleus. In Fig. 8 we plot (solid line) the distribution of mass, M_{inf}, accumulated in the centre of the halo up to redshift $z = 6$. The thin line corresponds to the same distribution inferred for those systems that host a BH, regardless of the fact that the BH is native or inherited, and irrespective to the formation channel. Systems at $z = 6$ have had time to accumulate a mass that covers a range from a few 10^3–10^4 $M_\odot$ to 10^8 $M_\odot$. Note that BH seeds are clustered in the high-mass tail of the M_{inf} distribution. This is suggestive of the fact that they can reach the mass range of supermassive BHs already at redshift $z \sim 6$. Note, however, that even assuming that all M_{inf} goes into growing a BH, BHs weighing billion solar masses are not present in our simulated volume, possibly because of its limited size. Very massive haloes are not statistically represented in our volumes. Given the number density of $z = 6$ QSOs, the number of BH with masses $>10^8$–10^9 $M_\odot$ expected in our cosmological volume is less than unity.

The novel channel of BH formation via runaway collisions in high-redshift pre-galactic discs, metal enriched by the first generation of PopIII stars, is a promising path for the formation of seeds. This holds true as long as metal enrichment and diffusion are mild, i.e. as long as the mean metallicity remains sufficiently low, such that runaway collisions can produce a VMS.

ACKNOWLEDGMENTS

REFERENCES

Alvarez M. A., Bromm V., Shapiro P. R., 2006, ApJ, 639, 621
Baker J. G., Boggs W. D., Centrella J., Kelly B. J., McWilliams S. T., Miller M. C., van Meter J. R., 2007, ApJ, 668, 1140
Bardeen J. M., Petterson J. A., 1975, ApJ, 195, L65
Begelman M. C., Volonteri M., Rees M. J., 2006, MNRAS, 370, 289
Belkus H., Van Bever J., Vanbeveren D., 2007, ApJ, 659, 1576
Bellovary J., Volonteri M., Governato F., Shen S., Quinn T., Wadsley J., 2011, ApJ, 742, 13
Bett P., Eke V., Frenk C. S., Jenkins A., Helly J., Navarro J., 2007, MNRAS, 376, 215
Bromm V., Loeb A., 2003, Nat, 425, 812
Bromm V., Ferrara A., Coppi P. S., Larson R. B., 2001, MNRAS, 328, 969
Callegari S., Mayer L., Kazantzidis S., Colpi M., Governato F., Quinn T., Wadsley J., 2009, ApJ, 696, L89
Campanelli M., Lousto C. O., Zlochower Y., Merritt D., 2007, Phys. Rev. Lett., 98, 231102
Carr B. J., 2003, Quantum Gravity: From Theory to Experimental Search, Vol. 631, p. Feedback from the First Stars and Galaxies and its Influence on Structure 301
Ciardi B., Ferrara A., 2005, Space Sci. Rev., 116, 625
Clark P. C., Glover S. C. O., Klessen R. S., 2008, ApJ, 672, 757
Clark P. C., Glover S. C. O., Klessen R. S., Bromm V., 2011, ApJ, 727, 110
Decarli R., Gavazzi G., Arosio I., Cortese L., Boselli A., Bonfanti C., Colpi M., 2007, MNRAS, 381, 136
Devecchi B., Volonteri M., 2009, ApJ, 694, 302 (DV09)
Devecchi B., Volonteri M., Colpi M., Haardt F., 2010, MNRAS, 409, 1057 (Paper I)
Dijkstra M., Haiman Z., Mesinger A., Wyithe J. S. B., 2008, MNRAS, 391, 1961
Dotan C., Rossi E. M., Shaviv N. J., 2011, MNRAS, 417, 3035
Dotti M., Volonteri M., Perego A., Colpi M., Ruszkowski M., Haardt F., 2010, MNRAS, 402, 682
Dunkley J. et al., 2009, ApJS, 180, 306
Eisenstein D. J., Loeb A., 1995, ApJ, 443, 11
Fan X. et al., 2001, AJ, 122, 2833
Fan X. et al., 2004, AJ, 128, 515
Ferrarese L., Merritt D., 2000, ApJ, 539, L9
Freese K., Bodenheimer P., Spolyar D., Gondolo P., 2008, ApJ, 685, 101
Freitag M., Gürkan M. A., Rasio F. A., 2006a, MNRAS, 368, 141
Freitag M., Rasio F. A., Baumgardt H., 2006b, MNRAS, 368, 121
Gallo E., Treu T., Jacob J., Woo J.-H., Marshall P. J., Antonucci R., 2008, ApJ, 680, 154
Gebhardt K. et al., 2000, ApJ, 539, L13
Glebbeek E., Gaburov E., de Mink S. E., Pols O. R., Portegies Zwart S. F., Glover S. C. O., Clark P. C., Greif T. H., Johnson J. L., Bromm V., Klessen R. S., Stacy A., 2009, in Hunt L. K., Madden S., Schneider R., eds, Proc. IAU 255 Open Questions in the Study of Population III Star Formation. Cambridge Univ. Press, Cambridge, p. 3
González J. A., Hannam M., Sperhake U., Brügmann B., Husa S., 2007, Phys. Rev. Lett., 98, 231101
Gültekin K. et al., 2009, ApJ, 698, 198
Gürkan M. A., Freitag M., Rasio F. A., 2004, ApJ, 604, 632
Haehnelt M. G., Rees M. J., 1993, MNRAS, 263, 168
Häring N., Rix H.-W., 2004, ApJ, 604, L89
Heger A., Woosley S. E., 2002, ApJ, 567, 532
Heger A., Fryer C. L., Woosley S. E., Langer N., Hartmann D. H., 2003, ApJ, 591, 288
Herrmann F., Hinder I., Shoemaker D. M., Laguna P., Matzner R. A., 2007, Phys. Rev. D, 76, 084032
Hirschi R., 2007, A&A, 461, 571
Iocco F., 2008, ApJ, 677, L1
Khlopov M. Y., 2010, Res. Astron. Astrophys., 10, 495
Kitayama T., Yoshida N., Susa H., Umemura M., 2004, ApJ, 613, 631
Koppitz M., Pollney D., Reisswig C., Rezzolla L., Thornburg J., Diener P., Schnetter E., 2007, Phys. Rev. Lett., 99, 041102
Koushiappas S. M., Bullock J. S., Dekel A., 2004, MNRAS, 354, 292
Lodato G., Natarajan P., 2006, MNRAS, 371, 1813
Lodato G., Natarajan P., 2007, MNRAS, 377, L64
Loeb A., Rasio F. A., 1994, ApJ, 432, 52
Machacek M. E., Bryan G. L., Abel T., 2001, ApJ, 548, 509
McKee C. F., Tan J. C., 2008, ApJ, 681, 771
Madau P., Rees M. J., 2001, ApJ, 551, L27

Magorrian J. et al., 1998, AJ, 115, 2285

Maio U., Ciardi B., Dolag K., Tornatore L., Khochfar S., 2010, MNRAS, 407, 1003

Maio U., Khochfar S., Johnson J. L., Ciardi B., 2011, MNRAS, 414, 1145

Mayer L., Kazantzidis S., Escala A., Callegari S., 2010, Nat, 466, 1082

Menou K., Haiman Z., Narayanan V. K., 2001, ApJ, 558, 535

Meynet G. et al., 2008, in Bresolin F., Crowther P. A., Puls J., eds, Proc. IAU Symp. 250, Massive Stars as Cosmic Engines. Cambridge Univ. Press, Cambridge, p. 571

Monaco P., Theuns T., Taffoni G., Governato F., Quinn T., Stadel J., 2002a, ApJ, 564, 8

Monaco P., Theuns T., Taffoni G., 2002b, MNRAS, 331, 587

Natarajan A., Tan J. C., O'Shea B. W., 2009, ApJ, 692, 574

O'Shea B. W., Norman M. L., 2008, ApJ, 673, 14

Omukai K., Palla F., 2003, ApJ, 589, 677

Omukai K., Tsuribe T., Schneider R., Ferrara A., 2005, ApJ, 626, 627

Omukai K., Schneider R., Haiman Z., 2008, ApJ, 686, 801

Perego A., Dotti M., Colpi M., Volonteri M., 2009, MNRAS, 399, 2249

Portegies Zwart S. F., McMillan S. L. W., 2002, ApJ, 576, 899

Portegies Zwart S. F., Makino J., McMillan S. L. W., Hut P., 1999, A&A, 348, 117

Portegies Zwart S. F., Baumgardt H., Hut P., Makino J., McMillan S. L. W., 2004, Nat, 428, 724

Prieto J., Padoan P., Jimenez R., Infante L., 2011, ApJ, 731, L38

Safranek-Shrader C., Bromm V., Milosavljevic M., 2010, ApJ, 723, 1568

Santoro F., Shull J. M., 2006, ApJ, 643, 26

Scannapieco E., Schneider R., Ferrara A., 2003, ApJ, 589, 35

Schaerer D., 2002, A&A, 382, 28

Schmidt M., 1959, ApJ, 129, 243

Schneider R., Ferrara A., Salvaterra R., Omukai K., 2004, BAAS, 36, 704

Schneider R., Omukai K., Inoue A. K., Ferrara A., 2006, MNRAS, 369, 1437

Schnittman J. D., 2007, ApJ, 667, L133

Schnittman J. D., Buonanno A., 2007, ApJ, 662, L63

Sijacki D., Springel V., Haehnelt M. G., 2009, MNRAS, 400, 100

Smith B. D., Turk M. J., Sigurdsson S., O'Shea B. W., Norman M. L., 2009, ApJ, 691, 441

Spaans M., Silk J., 2006, ApJ, 652, 902

Spolyar D., Freese K., Gondolo P., 2008, Phys. Rev. Lett., 100, 051101

Stacy A., Greif T. H., Bromm V., 2009, in Jogee S., Marinova I., Hao L., Blanc G., eds, ASP Conf. Ser. 419, Galaxy Evolution: Emerging Insights and Future Challenges. Astron. Soc. Pac., San Francisco, p. 339

Tanaka T., Haiman Z., 2009, ApJ, 696, 1798

Tegmark M., Silk J., Rees M. J., Blanchard A., Abel T., Palla F., 1997, ApJ, 474, 1

Toomre A., 1964, ApJ, 139, 1217

Tremaine S. et al., 2002, ApJ, 574, 740

Trenti M., Stiavelli M., 2009, ApJ, 694, 879

Turk M. J., Abel T., O'Shea B., 2009, Sci., 325, 601

Vink J. S., 2008, New Astron. Rev., 52, 419

Volonteri M., 2010, A&AR, 18, 279

Volonteri M., Begelman M. C., 2010, MNRAS, 409, 1022

Volonteri M., Rees M. J., 2006, ApJ, 650, 669

Volonteri M., Haardt F., Madau P., 2003, ApJ, 582, 559

Volonteri M., Lodato G., Natarajan P., 2008, MNRAS, 383, 1079

Volonteri M., Gültekin K., Dotti M., 2010, MNRAS, 404, 2143

Whalen D., Abel T., Norman M. L., 2004, ApJ, 610, 14

Whalen D., van Veelen B., O'Shea B. W., Norman M. L., 2008, ApJ, 682, 49

Wolcott-Green J., Haiman Z., Bryan G. L., 2011, MNRAS, 418, 838

Yoshida N., Abel T., Hernquist L., Sugiyama N., 2003, ApJ, 592, 645

Yungelson L. R., van den Heuvel E. P. J., Vink J. S., Portegies Zwart S. F., de Koter A., 2008, A&A, 477, 223

This paper has been typeset from a TeX/LaTeX file prepared by the author.